Dyes and Pigments 89 (2011) 271–277

Contents lists available at ScienceDirect

Dyes and Pigments

journal homepage: www.elsevier.com/locate/dyepig

Substrate induced catalysis: Deciphering the weak acid triggered bleaching of an angular terthiazole photochromic dye

T. Nagakawa [a], C.-L. Serpentini [b], C. Coudret [b,*], J.-C. Micheau [b], T. Kawai [a]

[a] Graduate School of Materials Science, NAIST, 8916-5 Takayama, Ikoma, Nara 630-0192, Japan
[b] Université de Toulouse, UPS, IMRCP, 118 route de Narbonne, F-31062, Toulouse Cedex 9, France

ARTICLE INFO

Article history:
Received 29 January 2010
Received in revised form
19 March 2010
Accepted 23 March 2010
Available online 31 March 2010

Keywords:
Photochromism
Diarylethenes
Terthiazole
Kinetic modeling
Acid catalysis

ABSTRACT

The thermal bleaching of the ring-closed colored isomer of a photochromic triangle terthiazole induced by a weak acid in acetonitrile was investigated from a kinetic point of view. A realistic model was proposed involving not less than nine species and thirteen elementary processes. Our studies highlight the importance of the transient monoprotonated species in the carbon–carbon bond weakening and confirm the role of the proton as catalyst for the ring opening. The origin of the sigmoid shape of the Absorbance *vs* time traces is discussed.

1. Introduction

The photoinduced reversible transformation of a molecule between two isomers exhibiting different absorption spectra is known as photochromism [1–3]. Azobenzenes, spirobenzopyrans, spironaphthooxazines and naphthopyrans show photoinduced coloration upon UV light irradiation and spontaneous backward bleaching to the initial isomers in the dark. They belong to the T-type as they are thermally reversible photochromic compounds. Some of them are currently used as the active materials in light-modulated sunglasses. On the other hand, the isomerisation of furylfulgides and diarylethenes is photochemically reversible but thermally irreversible. For such compounds, the commonly admitted isomerisation mechanism is a six π electrons electrocyclization and Woodward Hoffmann (WH) rules fully apply. This class of photochromic compound is known as the P-type. Such properties are useful for the future development of optoelectronic and photo-optical switching devices operating at the molecular and supramolecular levels such as memories, data storage devices. Most of the diarylethenes (DAE) bearing heterocyclic aryl groups such as thiophene or benzothiophenes belong to P-type photochromic compounds [4]. However, a thermal cycloreversion is not impossible, although not permitted by the WH rules. For instance, it is well-known that *cis*-stilbene (a hexatriene type molecule) undergoes photocyclization to form the thermally unstable dihydrophenanthrene which returns to stilbene in the dark in a deaerated solution: thus, *cis*-stilbene is a T-photochrom. The reason for this unstability was interpreted by the aromaticity loss underlying the isomerisation reaction [5]. But in some cases other subtle effects have been found to be superimposed. At first, the steric hindrance in the vicinity of the reactive carbon and DAE having bulky substituent groups on these positions show relatively unstable colored forms. Then indirect electronic factors have also been identified. Hence, when electron-withdrawing groups are introduced on dithienylethene derivatives (DTE), the closed isomer is known to be thermally less stable than if the substituents are electron-donating [6]. This property leads to DTE carrying "switchable" substituents, able to change from electron-donating to electron-withdrawing by oxidation [7] or by protonation [8].

Recently, it was shown that some compounds having their DTE "ethylene" double bond included in a conjugated moiety presented photochromic properties [9–11] and among them, angular terthiazole derived dyes have been studied (Scheme 1). In these compounds, the weak resonance energy of the thiazole ring leads to a ring-closed, blue colored form, stable at room temperature and for several hours at 100 °C [12].

Since there are three basic nitrogen atoms very close to the hexatriene core, an investigation of the influence of a moderate

* Corresponding author.
E-mail addresses: tkawai@ms.naist.jp (T. Nagakawa), coudret@chimie.ups-tlse.fr (C. Coudret).

0143-7208/$ – see front matter © 2010 Elsevier Ltd. All rights reserved.
doi:10.1016/j.dyepig.2010.03.024

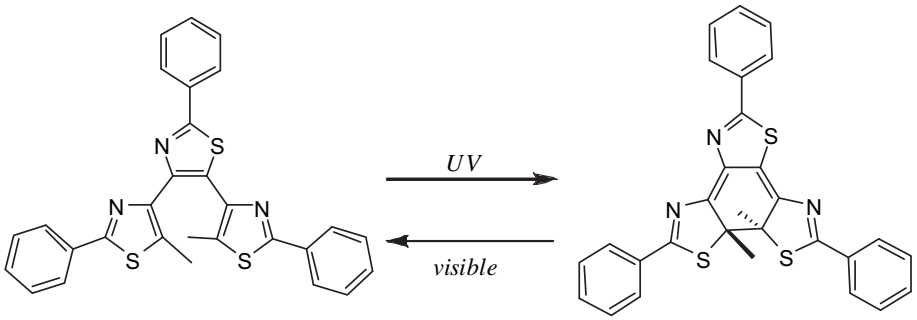

Scheme 1. P-photochromism of an angular terthiazole.

H^+ donor (trifluoroacetic acid (TFA) in acetonitrile) on the stability of the closed colored form was undertaken. In acetonitrile both isomers are very weak bases, but nonetheless we have shown that the interaction is sufficient to promote efficient ring opening. Although there is no spectroscopic evidence for the presence of protonated species, they may be present in quantities sufficient to trigger the ring opening reaction [13].

We think that such photochromic compounds are key molecules for the understanding of subtle organic chemical reaction dynamics. Therefore, the purpose of this paper is to undergo a careful kinetic analysis based on numerical simulation, multi-experiments curve fitting and parameters optimization using a home-made specific software to define the roles played by each species during the weak acid triggered bleaching of an angular terthiazole photochromic dye.

2. Experimental

2.1. Materials and methods

2.1.1. Products and solutions

Acetonitrile (HPLC grade, from SDS) and trifluoroacetic acid (Sigma) were used as received. Stock solutions of angular terthiazole (100–500 μM) were kept at room temperature, away from light. Stock solutions of TFA 1 M in acetonitrile were kept at room temperature no longer than a month.

2.1.2. Photostationary state generation

Before each experiment, the concentration of terthiazole solutions was checked by UV–visible spectrophotometry, at 326 nm (ε_{326} = 29 400 M^{-1} cm^{-1}). The solution was then placed in the thermostated sample holder of the spectrophotometer and irradiated at 313 nm until the absorbance monitored at 582 nm reached a plateau.

2.2. Kinetic recording of the TFA triggered bleaching of the closed form

After addition of the appropriate amount of trifluoroacetic acid (TFA), the cuvette was quickly shaken and placed in the spectrophotometer in which continuous magnetic stirring was maintained. Kinetic traces were acquired on an HP8451, diode array detector, single monochromator at 25 °C. Monitoring was achieved either by recording the entire absorption spectrum (on the 250–750 nm interval) or by monitoring the absorbance at 582 nm (λ_{max} of the colored form). In order to insure that there was no perturbation of the reaction rate by the measurement beam, kinetic tests have been made with and without a long pass filter (Schott GG3, 400 nm), with a short (10 s) or long (200 s) measurement interval, and with a short (0.2 s) or long (0.5 s and more) measurement time. The following initial conditions have been used: run A: $[TFA]_0 = 7 \times 10^{-5}$ M, $[O]_0 = 3.4 \times 10^{-5}$ M, $[C]_0 = 9.4 \times 10^{-6}$ M. Run B: $[TFA]_0 = 1.4 \times 10^{-5}$ M, $[O]_0 = 1.2 \times 10^{-5}$ M, $[C]_0 = 3.2 \times 10^{-5}$ M. Run C: $[TFA]_0 = 4.1 \times 10^{-5}$ M, $[O]_0 = 1.1 \times 10^{-5}$ M, $[C]_0 = 1.6 \times 10^{-5}$ M. Run D: $[TFA]_0 = 2.1 \times 10^{-5}$ M, $[O]_0 = 1.34 \times 10^{-5}$ M, $[C]_0 = 1.34 \times 10^{-5}$ M.

2.3. Kinetic data analysis

The recorded kinetic curves have been fitted using the "sa" program. Table 2 displays the list of processes occurring in the assumed model.

The corresponding set of differential equations is:

$$d[C]/dt = -v_0 + v_1 + v_{11} - v_{12};$$

$$d[AH]/dt = -v_0 + v_1 - v_2 + v_3 - v_9 + v_{10};$$

$$d[(C.AH)]/dt = v_0 - v_1 - v_4 + v_5;$$

$$d[O]/dt = -v_2 + v_3 - v_{11} + v_{12};$$

$$d[(O.AH)]/dt = v_2 - v_3 - v_6 + v_7;$$

$$d[CH^+]/dt = v_4 - v_5 - v_8 - v_{11} + v_{12};$$

$$d[A^-]/dt = v_4 - v_5 + v_6 - v_7 - v_9 + v_{10};$$

$$d[OH^+]/dt = v_6 - v_7 + v_{11} - v_{12} + v_8;$$

$$d[(AHA^-)]/dt = v_9 - v_{10};$$

The concentrations are controlled by three conservation equations.

Mass conservation of the dye:

$$[O]_0 + [C]_0 = [C] + [CH^+] + [(C.AH)] + [O] + [OH^+] + [(O.AH)]$$

Mass conservation of the trifluoroacetate moiety:

$$[AH]_0 = [A^-] + [AH] + [(C.AH)] + [(O.AH)] + 2[(AHA^-)]$$

and electroneutrality of the solution:

$$[A^-] + [(AHA^-)] = [CH^+] + [OH^+]$$

Beer's law is used for the calculation of the absorbance:

$$Abs = \varepsilon\ell([C] + [(C.AH)] + [CH^+])$$

where ε is the molar absorption coefficient of the closed form whatever its protonation or association state [14].

All the parameters were chosen randomly to start a fitting procedure. Then, they were refined by trial and error using a simulated annealing technique until a rather good fit was obtained. Finally, the parameters were optimized automatically using an iterative algorithm of the Powell type, designed to minimize the residual quadratic error $\chi^2 = \Sigma n \Sigma m\ (Ycal - Yobs)^2$ between the experimental and the calculated curves (n is the number of experimental data points per kinetic curve and m the number of kinetic curves). The iterative fitting procedure was repeated five times in order to check the reproducibility of the optimized parameters values.

2.4. NMR analysis of the TFA addition on the open form

The variations of the chemical shifts of Me2 protons available from a previous NMR study (see Scheme 2) have been used to analyze the stoichiometry of the TFA interaction with the open isomer in deuterated acetonitrile.

Three possible stoichiometries have been assumed. The corresponding global processes are gathered on Table 1.

In each of these processes, the open form of the dye appears in two species: the free base itself (O) and as a product resulting of the interaction with the acid: OH^+ in entries (1) and (2), or $(OH.AH)^+$ in entry (3). Considering that equilibria were fast enough an average chemical shift between these two species was introduced as:

$$\delta_{obs} = (\delta_O[O] + (\delta_{assoc}[assoc])/[O]_0$$

where δ_O is the chemical shift of the free open form O and δ_{assoc} that of the "associated" open form (noted "assoc" in the equation) OH^+ or $(OH.HA)^+$. $[O]_0$ is the initial concentration of the open form. The three parameters δ_O, δ_{assoc} and the equilibrium constant K_{NMR} were fitted simultaneous using our home-made "sa" software [15]. To do so, each reversible process was translated into a set of differential equations which were integrated numerically until the equilibrium state was reached. The equilibrium position is displaced by varying the concentration of added acid. Chemical shift is then calculated from the equilibrium concentrations of free and associated species (see Fig. 2).

3. Results and discussion

3.1. Kinetic runs

Numerical simulation and multi-experiment curve fitting has been used to obtain a comprehensive picture of the acid triggered bleaching of the closed form of the angular terthiazole. This methodology which employs long period UV/visible monitoring of the absorbance changes and numerical methods for the recorded data treatment is able to distinguish between different proposed mechanistic models and to analyse their validity from only a few number of experiments. The specificity of this approach is that we consider the whole kinetic curves from the start of the reaction to the equilibrium. Because there was no attempt to work in pseudo first order conditions or to use only the initial rates, our method takes advantage of the continuous variations of the substrate, intermediates and products during the course of the reaction. This added complexity is only apparent using the to-day available powerful computing tools which allow a careful analysis of the size, the shape, the curvature and the relative positions of the various kinetic traces recorded from a limited series of initial conditions. To explore these effects, the relative initial concentrations of the open (O) and closed (C) forms and the acid (TFA) were chosen in order that the $[C]_0/[O]_0$ and $[TFA]_0/[C]_0$ were varied as it is shown on Table 3.

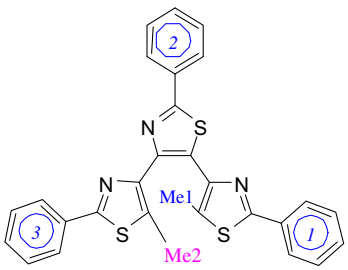

Scheme 2. Numbered structure of the angular terthiazole photochromic dye.

Table 1
Global reversible processes assumed for the analysis of equilibria between the open form (O) and trifluoroacetic acid (AH).

Stoichiometry	Global process
1	$O + AH = OH^+ + A^-$
2	$O + 2AH = OH^+ + (AHA)^-$
3	$O + 3AH = (OH.AH)^+ + (AHA)^-$

Kinetic traces are given on Fig. 1. At first sight, the decay is smooth in an apparent monotonous way. However, a careful look at the traces showed that most of them have a sigmoid shape: after an incubation time, the bleaching kinetics underwent acceleration. Such a feature is incompatible with a simple mechanism such as a first order one.

With such experiments in hands, we were able to process the data in order to get some of the kinetic parameters. It must be borne in mind that the global shape is bound to the slowest processes. In the present case, since a kinetic trace is typically recorded over more than 50 000 s an apparent global first order constant of ca 10^{-5} s^{-1} is expected. Faster processes are consequently hidden and no accurate description can be reached.

3.2. Homoconjugation of the trifluoroacetate anion

While the bleaching of the dye is obviously due to the presence of trifluoroacetic acid, it is likely that several species deriving from the closed colored or the open colorless dye should be involved. This assumption brings the focus on the properties of trifluoroacetic acid

Table 2
Mechanistic model of the acid-triggered ring opening of the closed terthiazole translated from the kinetic scheme on Fig. 3. Right column gathers the respective rate constants of the corresponding processes. All the equilibria are not independent since there are relationships which take into account of the detailed balance (see text).

List of processes	Rate of process	Rate constant of process
$C + AH \rightarrow (C.AH)$	$v_0 = k_1\ [C][AH]$	$k_1 = k_{-1}\ K_{ass}^{CAH}$
$(C.AH) \rightarrow C + AH$	$v_1 = k_{-1}[(C.AH)]$	k_{-1}
$O + AH \rightarrow (O.AH)$	$v_2 = k_{-5}[O][AH]$	$k_{-5} = k_5\ K_{NMR}/(K_{ion}^{OAH} K_{eq}^{AHA})$
$(O.AH) \rightarrow O + AH$	$v_3 = k_5[(O.AH)]$	k_5
$(C.AH) \rightarrow CH^+ + A^-$	$v_4 = k_2\ [(C.AH)]$	$k_2 = k_{-2}\ K_{ion}^{CAH}$
$CH^+ + A^- \rightarrow (C.AH)$	$v_5 = k_{-2}[CH^+][A^-]$	k_{-2}
$(O.AH) \rightarrow OH^+ + A^-$	$v_6 = k_{-4}[(O.AH)]$	$k_{-4} = k_4\ K_{ion}^{OAH}$
$OH^+ + A^- \rightarrow (O.AH)$	$v_7 = k_4[OH^+][\ A^-]$	k_4
$CH^+ \rightarrow OH^+$	$v_8 = k_3[CH^+]$	k_3
$AH + A^- \rightarrow (AHA^-)$	$v_9 = k_7[AH][A^-]$	$k_7 = k_{-7}\ K_{eq}^{AHA}$
$(AHA^-) \rightarrow AH + A^-$	$v_{10} = k_{-7}[(AHA^-)]$	k_{-7}
$CH^+ + O \rightarrow C + OH^+$	$v_{11} = k_{-6}[CH^+][O]$	$k_{-6} = k_6\ K_{NMR}/(K_{eq}^{AHA}\ K_{ass}^{CAH}\ K_{ion}^{CAH})$
$C + OH^+ \rightarrow CH^+ + O$	$v_{12} = k_6[C][OH^+]$	k_6

Table 3
Experimental design of the kinetic runs for the acid induced bleaching of the closed form. $1.1 \times 10^{-5} < [O]_0 < 3.4 \times 10^{-5}$ M; $0.3 < [C]_0/[O]_0 < 2.7$; $0.4 < [TFA]_0/[C]_0 < 7.5$. Number of crosses indicates the level of each constraint in the given interval (scale is: ++++: high; +: low).

Experiments	$[O]_0$	$[C]_0/[O]_0$	$[TFA]_0/[C]_0$
A	++	+	++++
B	+	++++	+
C	+	+++	+++
D	+	++	++

in acetonitrile as well as on the extent of the acido-basic reactions of both photoisomers. Indeed, with a high dielectric constant (37.5) but a rather average donor number (14.1) [16], acetonitrile is known as a protophobic solvent. Thus, Broensted acids tend to be weaker in acetonitrile than in water. However, protic acids and bases in acetonitrile can associate yielding larger hydrogen-bounded complexes. When an acid associates to its conjugated base, the resulting ion is called a "homoconjugated ion".

$$A^- + AH = (AHA)^- \; K_{eq}$$

The resulting stabilization of the conjugated base can pull ionization equilibria at the expense of the free acid or of hydrogen-bonded complexes [17]. Homoconjugation equilibrium constants (K_{eq}) have been determined for some acidic species including trifluoroacetic acid [18]. Consequently, new acid derived species, the homoconjugated ion $[(CF_3CO_2)_2H]^-$ (noted $(AHA)^-$) should be introduced in the models. This prompted us to refine the previously recorded NMR data concerning the interaction between the O form and TFA.

3.3. Open form/TFA interaction

As it was stressed in our previous paper, the titration of the open form O with trifluoroacetic acid gives rise to a very soft equilibrium, even in the large range of explored TFA-to-open form initial ratio (from 0 to 30 eq). Hence, in a first attempt, the data were analyzed according to the simplest 1:1 stoichiometry for the titration reaction by linearization in a double reciprocal plot. This is why we concluded

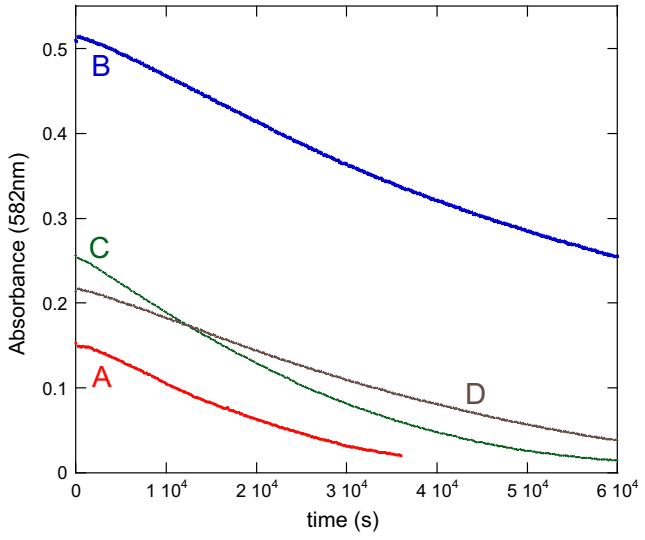

Fig. 1. Evolution of the absorbance during the acid triggered thermal bleaching of the terthiazole in acetonitrile solution at 25 °C. See text for the initial conditions of the A, B, C, and D runs. Experiments and fittings are superposed.

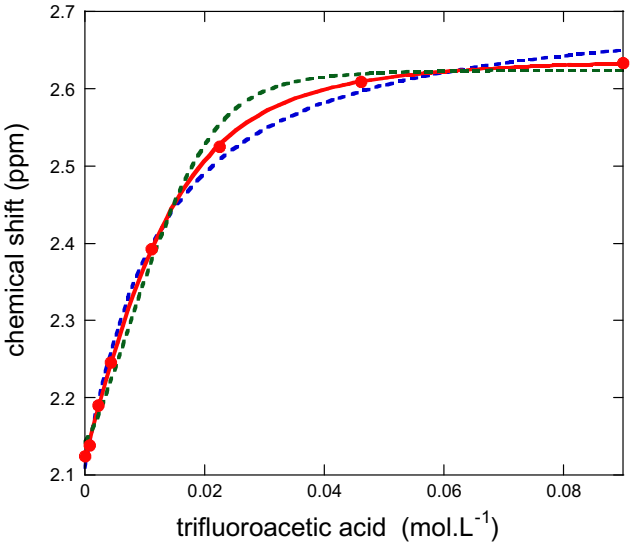

Fig. 2. Changes of the observed signals of the methyl-2 (nitrogen side) in the ^{1}H NMR spectrum of the open terthiazole O upon addition of TFA in CD_3CN at room temperature; $[O]_{tot.} = 3 \times 10^{-3}$ M. Red continuous curve is the best fit assuming an $O + 2AH = OH^+ + (AHA)^-$ model. $K^{1:2}_{NMR} = 26.6\ M^{-1}$.Blue dashed line corresponds to the $O + AH = OH^+ + A^-$ equilibrium. Green dashed line to the $O + 3AH = (OH.HA)^+ + (AHA)^-$ equilibrium.

that a (O.AH) hydrogen-bonded complex was present. However, such a treatment is known to cluster the points obtained at high concentration, and to give more weight to the low concentration points, thus possibly leading to heavy distortion. In light of the possible assistance of another acid molecule for the ionization of the (O.AH) complex, we have reexamined the collected data questioning the proposed equilibrium stoichiometry, but still considering that the ionization of TFA in acetonitrile (leading to solvated H^+) was negligible. Thus a direct approach was applied considering the presence of homoconjugated ion $(AHA)^-$ and the possibility of multiple associations to the open form as it exhibits 2 basic sites. 1:1, 1:2 and 1:3 stoichioimetries were thus tested, keeping in mind that only the open forms were probed by the ^{1}H NMR. Fig. 2 shows that the best fit was obtained by considering a 1:2 stoichiometry.

The best fit indicated a 1:2 stoichiometry. This result rules-out the possibility of having the associated species (O.AH) as the major species, but also points out the weak basicity of the thiazole ring: a double protonation that could be expected at high TFA concentrations would indeed require a higher stoichiometry. This is supported by the rare data available on this heterocycle in water: with a pK_a of 3.40, 2-methylthiazole is a very poor base in water [19], and according to studies run of pyridinic bases, transfer to ACN should not improve it [20].

Moving to a mechanistic description, the global equilibrium observed by NMR, having a molecularity of 3, was considered as the result of three coupled equilibria. Therefore its equilibrium constant K_{NMR} was rewritten as a function of some elementary equilibria: the association of the O species with trifluoroacetic acid to give the H-bonded complex (O.AH):

$$O + AH \leftarrow\ \rightarrow (O.AH)\ K^{(OAH)}_{ass} = k_{-5}/k_5$$

the subsequent complex ionization giving rise to OH^+ and A^-:

$$(O.AH) \leftarrow\ \rightarrow OH^+ + A^-\ K^{(OAH)}_{ion} = k_{-4}/k_4$$

and the already mentioned homoconjugation equilibrium (K_{eq}).

$AH + A^- \leftarrow\rightarrow (AHA)^- \; K_{eq} = k_7/k_{-7}$

One could easily derive the following formula for K_{NMR} for the 1:2 stoichiometry

$O + 2AH = OH^+ + (AHA)^- \; K_{NMR} = K_{ass}^{(OAH)}.\, K_{ion}^{(OAH)}.K_{eq}$

3.4. Establishment of mechanistic scheme

The closed isomer C was assumed to participate to a set of analogous equilibria: a first giving rise to the associated complex (C.AH) ($K_{ass}^{(CAH)} = k_1/k_{-1}$) and its ionization to give the cation CH^+ ($K_{ion}^{(CAH)} = k_2/k_{-2}$) (see Experimental part for more details).

Moreover, a last equilibrium describing the possible exchange of a proton between the two forms independently of any of the trifluoroacetic acid derived species has been considered. This process corresponds to a cross reaction between the protonated and neutral forms of both isomers:

$C + OH^+ = CH^+ + O \; K_{cross} = k_6/k_{-6}$

Its equilibrium constant can be expressed as a function of the aforementioned elementary equilibria, or as a function of the constant K_{NMR}. We have:

$K_{cross} = (K_{ion}^{(CAH)}.K_{ass}^{(CAH)})/(K_{ion}^{(OAH)}.K_{ass}^{(OAH)}) = (K_{ion}^{(CAH)}.K_{ass}^{(CAH)}.\, K_{eq})/K_{NMR}$

From all these considerations, the following mechanistic scheme was assumed. It involves nine species and thirteen elementary processes, most of them being reversible. Only the ring opening reaction (k_3) was declared irreversible.

Using known or independently measured parameters ($K_{eq} = 1.5 \times 10^{-4}$ M^{-1}; $K_{NMR} = 26.6$ M^{-1}) and starting with different sets of assay random parameters, the curve fitting processes converged repeatedly (see Fig. 1) allowing us to extract some characteristic kinetic parameters or features. Among them, three second-order and one first order rate constants have been obtained with a satisfactory accuracy. The results are gathered in the Table 4:

Other kinetic parameters have not been reached with a sufficient precision to be displayed in a table. The reason is that they are too rapid (or too slow) to influence our kinetic runs in the 10^4 s time window. Among the rapid first order rate constants there are:

$(C.AH) \rightarrow C + AH \; (k_{-1})$, $(C.AH) \rightarrow CH^+ + A^- \; (k_2)$, $(O.AH) \rightarrow O + AH \; (k_{-5})$

and $(O.AH) \rightarrow OH^+ + A^- \; (k_{-4})$, and among the rapid second-order rate constants there are:

$CH^+ + A^- \rightarrow (C.AH) \; (k_{-2})$ and $O + AH \rightarrow (O.AH) \; (k_5)$.

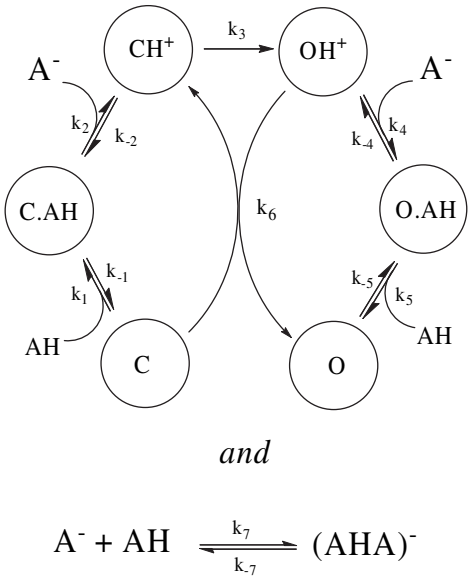

Fig. 3. Kinetic scheme showing the assisted protonation of both the closed C and open form O, the ring opening of the protonated closed form CH^+ and the proton exchange reaction between the protonated open form OH^+ and the free closed form C. For the later process, the back reaction (rate constant k_{-6}) has not been shown for sake of clarity.

On the other side, the reverse of the proton exchange $CH^+ + O \rightarrow C + OH^+$ (k_{-6}) is certainly very slow and has been neglected.

With the computer program used it is possible to add or suppress processes. For instance, the possibility of a direct conversion between the neutral associated species (C.AH) → (O.AH) has been ruled-out. This result confirms the role of the fully protonated species in the overall transformation. Several other possible processes have also been eliminated such as spontaneous trifluoroacetic acid dissociation in acetonitrile, direct dye protonation and exchange reaction within the neutral dye/TFA associates. From all these considerations it can be stated that the proposed model is the more likely, although it cannot be excluded that the extracted parameters could be more or less model-dependent.

It can be instructive to look at the time evolution of the various species (see Fig. 4).

Although all the processes are occurring simultaneously, it is possible to distinguish periods during which one given process is primordial. At the beginning of the bleaching, the main process is: $C \rightarrow CH^+$. The initial slope of C is $\approx 1.5 \times 10^{-9}$ M s^{-1} close to $k_1[C][AH] = 3.4 \times 3.2 \times 10^{-5} \times 1.4 \times 10^{-5} = 1.52 \times 10^{-9}$M s^{-1}. Then, at the end of the plot, the slope of the decay of C is $\approx 1.6 \times 10^{-10}$ M s^{-1}. At this time, the contribution of $CH^+ \rightarrow OH^+$ which is $k_3[CH^+] \approx 6.1 \times 10^{-5} \times 2.5 \times 10^{-6} = 1.5 \times 10^{-10}$ M s^{-1} indicates that this is the main operating process for the ring opening. On the other hand, overall processes such as $OH^+ \rightarrow O$ and $C \rightarrow O$ are likely to also occur at the same time. Looking at the acid derived species

Table 4
List of processes with their respective rate constants extracted from the kinetic curve fittings. All of them exhibit an apparent pseudo first order rate constant around 5×10^{-5} s^{-1} roughly matching the time window of our kinetic runs ($\approx 2 \times 10^4$ s).

Processes	Rate constants	Unit	Pseudo 1st order rate constant
$C + AH \rightarrow (C.AH)$	$k_1 = 3.4 \pm 0.2$	M^{-1} s^{-1}	$k_1[AH] \approx 3.4{*}4 \times 10^{-6} \approx 1.4 \times 10^{-5}$
$A^- + OH^+ \rightarrow (O.AH)$	$k_4 \approx 10 \pm 6$	M^{-1} s^{-1}	$k_4[A^-] \approx 10{*}7 \times 10^{-6} \approx 7 \times 10^{-5}$
$C + OH^+ \rightarrow CH^+ + O$	$k_6 = 0.45 \pm 0.3$	M^{-1} s^{-1}	$k_6[OH^+] \approx 0.45{*}7 \times 10^{-6} \approx 3.1 \times 10^{-5}$
$CH^+ \rightarrow OH^+$	$k_3 = 6.1 \times 10^{-5}$	s^{-1}	$k_3 = 6.1 \times 10^{-5}$

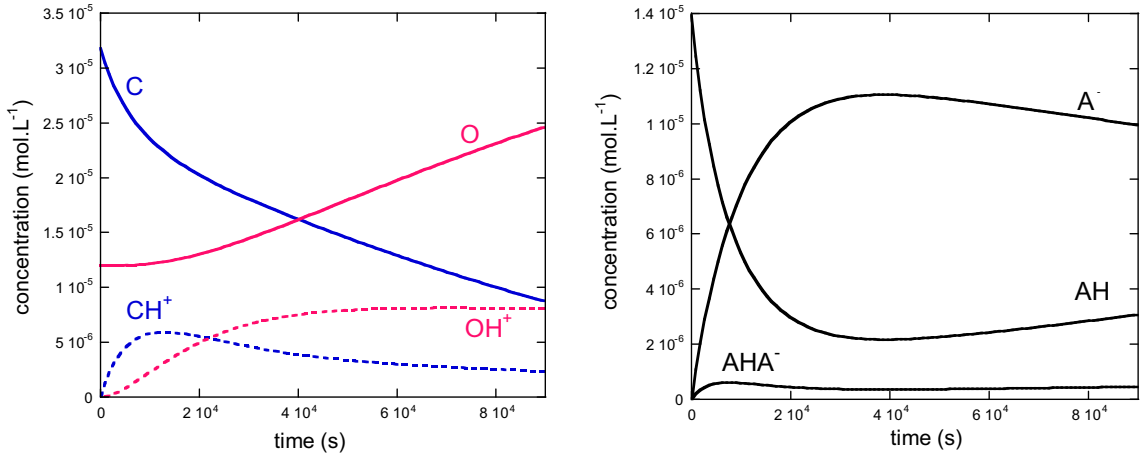

Fig. 4. Simulated evolution of the concentrations of the various species during the ring opening process of the terthiazole in presence of TFA in run B. (O.AH) and (C.AH) are not plotted as their concentrations remains always negligible.

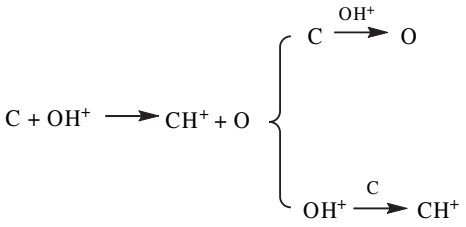

Scheme 3. Net effect of the proton cross-exchange reaction, either a ring-opening driven by the protonated open form (top) or a ring closure driven by the closed form (bottom).

shows that the time evolution of the concentrations of anions A^- and $(AHA)^-$ are complex unveiling their coupling with the multi-equilibria decay of the closed form.

Two important slow reactions have a strong impact on the global bleaching kinetics: the ring opening reaction $CH^+ \rightarrow OH^+$ and the H^+ cross-exchange namely: $C + OH^+ \rightarrow CH^+ + O$. These two reactions are totally different in terms of mechanism but play an important role in the time evolution of the protonated forms concentration. In particular, the proton cross- exchange can be considered from two points of view as it is displayed in the Scheme 3.

From the top one, the overall result is the conversion of the closed neutral species C into the open one. This process necessitates some OH^+ species, that is to say a product-activated process. This reading is very reminiscent of an autocatalytic reaction. The other point of view (bottom) is more subtle: it can be seen as the reverse of the ring opening reaction but driven by the closed form C. In other words, the substrate C slows down the building-up of OH^+, it inhibits the ring opening. This reading is very reminiscent of a substrate-inhibition. As a consequence, the global coupling between ring opening and cross-protonation gives rise to a non-linear effect (autocatalysis + substrate-inhibition) responsible of the sigmoïdal shape of the kinetic traces.

4. Conclusion

The UV–vis kinetic monitoring of the trifluoroacetic acid bleaching of the colored (ring-closed) form of the angular terthiazole photochromic dye as well as the NMR titration of the colorless (ring-open) one were carefully reexamined. The approach used is based on numerical modeling, data analysis and multi-experiments curve fitting. This technique was applied to treat either equilibrium (titration) or time dependent (kinetic traces) data. Its interest relies on the fact that very few assumptions but the mechanistic steps and species are necessary. Applied to the present problem, this method enabled us to show that at least 9 species were necessary, and among them, the fully protonated species played a decisive role: indeed the carbon–carbon bond cleavage occurs only once the terthiazole dye is protonated. Furthermore it also emphasize the role of the protophobic solvent, since homoconjugated ions derived from the acid must be introduced to interpret the experimental results.

The avoidance of pseudo first order conditions allowed us to highlight some non-linear kinetic effects occurring during the dye bleaching. The proposed mechanism reproduces the sigmoid shape of the kinetic traces thanks to the coupling between two slow reactions: the bond breakage step and the cross-protonation one between the terthiazole species. While the first one is unimolecular involving the protonated species, the second is essentially bimolecular, concerning both the reactant and the product of the transformation. When the conversion has reached a threshold, the rate of the bimolecular process becomes of the same order of magnitude of the unimolecular one. This matching causes a slight variation of the rate of the global bleaching process leading to the observed sigmoid shape.

The modeling has also revealed that ring closure of the terthiazole enhances its basicity. The origin of this feature is beyond the scope of this study but several tracks can be proposed: the obvious global electronic reorganization but also the geometrical changes that accompany the cyclization. In particular the rigidity of closed isomer locks the nitrogen lone pairs in a defined direction.

Eventually the main result obtained is the more accurate value for the C–C bond breaking rate constant: the value obtained 6.1×10^{-5} s^{-1} is still much higher than the room temperature uncatalyzed one ($\approx 6.6 \times 10^{-9}$ s^{-1} at 25 °C).

The proton cross-exchange step brings a new aspect of the transformation: this step can be viewed as a “propagative” process in which the actual catalyst, the proton, is transferred from the product OH^+ to the reactant C. Associated to the fact that acid ionization is due to the reaction with the basic dye, it illustrates how the substrate is inducing the catalysis that causes its disappearance. Such a phenomenon would not have been evidenced if a stronger acid had been used.

Acknowledgements

The authors thank the NAIST-Université de Toulouse, Paul Sabatier Exchange Program for a grant (T. N). This work was supported in part by the CNRS, France, in part by the Ministry of

Education, Culture, Sports, Science and Technology (MEXT), Japan: Grants-in-Aid for Scientific Research (B) (No. 17350069) and Scientific Research on Priority Areas, “Super-Hierarchy Structures” (No. 17067011).

References

[1] Irie M. Chem Rev 2000;100:1685–716.
[2] Tian H, Yang S. Chem Soc Rev 2004;33:85–97.
[3] Matsuda K, Irie M. J Photochem Photobiol C: Photochem Rev 2004;5:169–82.
[4] Kobatake S, Irie M. Annu Rep Prog Chem Sect C 2003;99:277–313.
[5] Nakamura S, Yokojima S, Uchida K, Tsujioka T, Goldberg A, Murakami A, et al. Photochem Photobiol A: Chem 2008;200:10–8.
[6] Gilat SL, Kawai SH, Lehn J-M. Chem Eur J 1995;1:275–84.
[7] Guirado G, Coudret C, Launay J-P. J Phys Chem C 2007;111:2770–6.
[8] Kobatake S, Terakawa Y. Chem Commun; 2007:1698–700.
[9] Zhu W, Meng X, Yang Y, Zhang Q, Xie Y, Tian H. Chem Eur J 2010;16:899–916.
[10] Ko CC, Kwok WM, Yam VWW, Phillips DL. Chem Eur J 2006;12:5840–8.
[11] Kawai T, Iseda T, Irie M. Chem Commun; 2004:72–4.
[12] Nakashima T, Atsumi K, Kawai S, Nakagawa T, Hasegawa Y, Kawai T. Eur J Org Chem; 2007:3212–8.
[13] Coudret C, Nakagawa T, Kawai T, Micheau J-C. New J Chem 2009; 33:1386–92.
[14] The same molar extinction coefficient (ε_{582} = 16,000 M^{-1} cm^{-1}) has been used for C, (C.AH) and CH+ as no UV/visible change was observed even after addition of a large excess of TFA.
[15] For a chemical kinetics tutorial and “sa” software downloading, the reader is invited to visit the following web site: http://pagesperso-orange.fr/cinet.chim/index.html.
[16] Reimers JR, Hall LE. J Am Chem Soc 1999;121:3730–44.
[17] Wang LY, Wu CA, Chen YF, Wang SL. J Chin Chem Soc 2006;53:1463–8.
[18] Pawlak M, Tusk S, Kuna F, Rohbusch MF, Fox F. J Chem Soc. Faraday Trans 1 1984;80:1757–68.
[19] Güray T, Açikkalp E, Ogretir C, Yarligan S. J Mol Graph Model 2007; 26:154–65.
[20] Augustin-Nowacka D, Chmurzynski L. Anal Chim Acta 1999;381:215–20.